

## Proton-exchange membrane regenerative fuel cells

Larry L. Swette, Anthony B. LaConti and Stephen A. McCatty  
Giner, Inc., 14 Spring Street, Waltham, MA 02154-4497 (USA)

### Abstract

This paper will update the progress in developing electrocatalyst systems and electrode structures primarily for the positive electrode of single-unit solid polymer proton-exchange membrane (PEM) regenerative fuel cells. The work was done with DuPont Nafion 117 in complete fuel cells (40 cm<sup>2</sup> electrodes). The cells were operated alternately in fuel cell mode and electrolysis mode at 80 °C. In fuel cell mode, humidified hydrogen and oxygen were supplied at 207 kPa (30 psi); in electrolysis mode, water was pumped over the positive electrode and the gases were evolved at ambient pressure. Cycling data will be presented for Pt–Ir catalysts and limited bifunctional data will be presented for Pt, Ir, Ru, Rh and Na<sub>x</sub>Pt<sub>3</sub>O<sub>4</sub> catalysts as well as for electrode structure variations.

### Introduction

In prior work [1–3], a large number of candidate bifunctional positive electrode catalysts were evaluated for chemical and electrochemical stability and for catalytic activity in 30% KOH at 80 °C. As a result of this work, two potentially bifunctional catalyst systems were identified: (i) Na<sub>x</sub>Pt<sub>3</sub>O<sub>4</sub> [4] and (ii) metal/metal oxide combinations of Rh, Pt and Ir [3]. More recently the scope of the program was expanded to include development of bifunctional positive electrode catalysts for the regenerative proton-exchange membrane (PEM) fuel cell, focusing on many of the same catalysts.

In order to alternate between O<sub>2</sub> reduction and O<sub>2</sub> evolution on the same electrode, in addition to bifunctional catalysis, it is necessary to have an electrode structure that can perform in both of these modes. Some of the effort on this program was directed to the development of such structures. The approach taken was to develop catalyst/binder compositions optimized separately at the particulate level for either O<sub>2</sub> reduction (more hydrophobic) or O<sub>2</sub> evolution (more hydrophilic) and then combine these at an optimal ratio in a single electrode, referred to as an 'integrated dual-character' (IDC) electrode. In this approach the catalyst for each function can be the same material if it shows bifunctional activity (e.g. Na<sub>x</sub>Pt<sub>3</sub>O<sub>4</sub>), or two different monofunctional catalysts (e.g., Pt for O<sub>2</sub> reduction and IrO<sub>2</sub> for O<sub>2</sub> evolution). This approach, developed for the alkaline system, was extended to the PEM regenerative fuel cell by introducing a two-layer structure to achieve an appropriate interface to the more confined two-dimensional character of the proton-exchange membrane.

### Experimental

#### *Catalyst materials*

Platinum black, used in both the positive and negative electrode structures, was fuel cell grade material obtained from Engelhard Industries. Metal oxide catalysts

were prepared by proprietary modifications of Adams-type fusions of the metal salts in a nitrate flux [5]; metal/metal oxide catalysts ( $\text{Pt-MO}_x$ ) were prepared by cofusion of the metal salts in a similar manner followed by electrochemical reduction of the  $\text{PtO}_2$  to Pt, or were blends of separately prepared materials ( $\text{Pt-Na}_x\text{Pt}_3\text{O}_4$ ).

$\text{Na}_x\text{Pt}_3\text{O}_4$  was typically prepared by firing mixtures of  $\text{Na}_2\text{CO}_3$  and  $\text{PtO}_2$  under oxygen at 650 °C or higher for several hours. In most cases it was necessary to use a proprietary activation procedure to develop significant catalytic activity and acceptable conductivity.

The surface areas of all materials were determined by the BET nitrogen adsorption method using a Micromeritics Flowsorb II 2300 instrument. The electrical conductivities of materials were estimated by a two-point method measuring the resistance of the powders under moderate compression [2]. The compositions of the metal oxides prepared by nitrate fusion were determined in earlier work by X-ray diffraction analysis (XRD). Iridium chloride fusions yield  $\text{IrO}_2$ , which becomes slightly oxygen deficient  $\text{IrO}_{2-x}$  ( $x \sim 0.05$ ) if electrochemically reduced. Rhodium chloride fusions yield  $\text{RhO}_2$ . The ruthenium salt fusions yield  $\text{RuO}_2$ , which also becomes oxygen deficient  $\text{RuO}_{2-x}$  ( $x \sim 0.1$ ) if electrochemically reduced. The  $\text{Na}_x\text{Pt}_3\text{O}_4$  preparations were also analyzed by XRD for chemical characterization and determination of phase purity. The sodium content in  $\text{Na}_x\text{Pt}_3\text{O}_4$  can be determined from the unit cell parameter,  $a_0$ ,  $x = (a_0 - 5.59)/0.11$ . Recent preparations of  $\text{Na}_x\text{Pt}_3\text{O}_4$  have exhibited moderate surface areas and marginally acceptable conductivities without any post-synthesis treatment, and have been tested in that form. Materials characterization data are summarized in Table 1.

#### *PEM regenerative fuel cell testing*

A rechargeable fuel cell requires: (i) a negative electrode that is active for both  $\text{H}_2$  oxidation and  $\text{H}_2$  evolution, and (ii) a positive electrode that is active for both  $\text{O}_2$  reduction and  $\text{O}_2$  evolution. The general approach to achieve bifunctional electrode structures was to partially distribute the charge and discharge functions to separate catalyst layers of a composite electrode each of which is optimized primarily for one function. A hydrophilic PEM-bonded layer supports the gas-evolution functions; for  $\text{O}_2$  evolution the selected catalyst, at a loading of 1–3  $\text{mg}/\text{cm}^2$ , was blended with 10–20 wt.% of the ionomer and pressed onto the surface of the membrane. The gas-consumption discharge functions are supported by a separate more hydrophobic catalyst layer which was physically pressed against the PEM-bonded layer by the mechanical compression of the cell assembly.

Platinum is a good catalyst for the negative electrode reactions in both alkaline and acid electrolytes. We used the composite electrode structure for most of the PEM cell configurations. For the negative electrode the combination consisted of a platinum layer bonded directly to the PEM (optimized for  $\text{H}_2$  evolution) and a separate IDC electrode (optimized for  $\text{H}_2$  oxidation). The 'free-standing' component of the composite electrode consisted of an IDC platinum composition bonded to wet-proofed carbon paper.

The requirements for the positive electrode are more difficult to meet because of the scarcity of efficient bifunctional  $\text{O}_2$  catalysts. In addition, a titanium current collector is required because carbon support materials are not stable under  $\text{O}_2$ -evolution conditions. Platinum is an excellent  $\text{O}_2$ -reduction catalyst for the fuel-cell mode, but is relatively poor for  $\text{O}_2$  evolution.  $\text{IrO}_2$  is an excellent  $\text{O}_2$ -evolution catalyst, but a poor  $\text{O}_2$ -reduction catalyst. For electrolysis cells it is mixed or alloyed with Pt to improve the conductivity of the  $\text{IrO}_2$ . The general approach was to use Pt black for

TABLE 1

PEM regenerative fuel cell positive electrode: composition and characteristics of PEM-bonded layer

Cell #	Catalyst	Ratio (wt.%)	Loading (mg/cm <sup>2</sup> )	Ionomer (wt.%)	Surface area (m <sup>2</sup> /g)
5	Pt-IrO <sub>x</sub>	40-60	1	10	104
6	Pt overlay	33	1	0	28
	Na <sub>x</sub> Pt <sub>3</sub> O <sub>4</sub> #21 <sup>a</sup>	67	2	10	12
7	Na <sub>x</sub> Pt <sub>3</sub> O <sub>4</sub> #34A3 <sup>a</sup>	100	2	10	7
8	Pt-IrO <sub>x</sub>	40-60	1	15	117
9	RuO-IrO <sub>x</sub>	50-50	2	25	114
10	Pt-RuO <sub>x</sub>	40-60	1	15	69
11	RhO <sub>2</sub>	100	1	18	224
12	Pt-IrO <sub>x</sub>	40-60	1	10	117
13	Pt-IrO <sub>x</sub>	40-60	1	10	117
14	Pt black + Na <sub>x</sub> Pt <sub>3</sub> O <sub>4</sub> #41 <sup>a</sup>	33	1	10	29
		67	2	10	18
15	Pt black + Na <sub>x</sub> Pt <sub>3</sub> O <sub>4</sub> #43 <sup>a</sup>	33	1	10	29
		67	2	10	35
16	Pt black + Na <sub>x</sub> Pt <sub>3</sub> O <sub>4</sub> #43 <sup>a</sup>	33	1	10	29
		67	2	10	35

<sup>a</sup>Na<sub>x</sub>Pt<sub>3</sub>O<sub>4</sub> characteristics.

Preparation #	Surface area (m <sup>2</sup> /g)	Conductivity (Ω cm <sup>-1</sup> )	Unit cell parameter	Na <sub>x</sub> value
#21	12	33	5.671(3)	0.74
#34A3	7	30	5.674(1)	0.76 ('activated')
#41	18	0.3	5.675(3)	0.77
#43	35	3.4	5.688(1)	0.89

the O<sub>2</sub>-reduction function in the free-standing component and to incorporate the more favorable O<sub>2</sub>-evolution catalyst in the PEM-bonded layer, with Pt added to improve conductivity. For baseline performance data we used Pt or Pt-IrO<sub>2</sub> as the O<sub>2</sub>-electrode catalyst. Three baseline cell types were fabricated and tested: a Pt/Pt fuel cell (also tested as an electrolyzer), a Pt/Pt-IrO<sub>2</sub> electrolyzer, and several Pt/Pt-IrO<sub>2</sub> bifunctional cell configurations; subsequently, Pt/Pt-Na<sub>x</sub>Pt<sub>3</sub>O<sub>4</sub> bifunctional cells of similar construction were also tested [6]. More recently, as the O<sub>2</sub>-evolution catalyst, we have evaluated Pt-RuO<sub>x</sub>, RuO<sub>x</sub>-IrO<sub>x</sub> and RhO<sub>2</sub>, and we examined the performance of Pt-IrO<sub>x</sub> and Na<sub>x</sub>Pt<sub>3</sub>O<sub>4</sub> with repeated cycling.

The baseline Pt/Pt fuel cell and the experimental bifunctional cells were fabricated with a Nafion 117 PEM and utilized composite electrodes (catalyst layer bonded to the PEM plus a free-standing IDC electrode) on both sides. The baseline fuel cell and all of the experimental bifunctional cells had the same negative (H<sub>2</sub>) electrode

configuration. On the  $O_2$  side, the PEM-bonded electrode was Pt, Pt-IrO<sub>2</sub>, Pt-RuO<sub>x</sub>, RuO<sub>x</sub>-IrO<sub>x</sub>, RhO<sub>2</sub> or Pt-Na<sub>x</sub>Pt<sub>3</sub>O<sub>4</sub>, and the free-standing electrode was Pt or Pt-Na<sub>x</sub>Pt<sub>3</sub>O<sub>4</sub> on titanium mesh (Pt-plated). The baseline electrolysis cell had only the PEM-bonded electrode layers, optimized for gas evolution only (without ionomer added). In electrolysis mode, the cells were run at ambient pressure with heated water pumped through the positive electrode chamber; in fuel-cell mode the gases were supplied at 207 kPa and the H<sub>2</sub> stream was humidified at 90–120 °C. The majority of testing was done at a cell temperature of 80 °C.

## Results

As described above, three different types of PEM cells were constructed and tested to establish a performance baseline for single-function cells (fuel cell or electrolyzer) and a bifunctional cell. Subsequently, bifunctional PEM cells with Pt-Na<sub>x</sub>Pt<sub>3</sub>O<sub>4</sub> positive electrodes were fabricated and tested to determine the relative performance of this potential catalyst in acid electrolyte. More recently we have evaluated Pt-RuO<sub>x</sub>, RhO<sub>2</sub> and RuO<sub>x</sub>-IrO<sub>x</sub> as the O<sub>2</sub>-evolution components in bifunctional cells and investigated the performance of Pt-IrO<sub>x</sub> and Pt-Na<sub>x</sub>Pt<sub>3</sub>O<sub>4</sub> under limited cycling conditions.

### Baseline cells

#### Baseline Pt/Pt fuel cell

In fuel-cell mode, this cell ran at 0.874 V at 100 mA/cm<sup>2</sup> and at 0.714 V at 500 mA/cm<sup>2</sup> at 80 °C. As an electrolyzer, performance was poor, as expected, primarily because Pt is not a very good catalyst for O<sub>2</sub> evolution: 1.77 V at 100 mA/cm<sup>2</sup>, 2.00 V at 500 mA/cm<sup>2</sup> at 80 °C. This cell was provided with the same positive electrode structure as used in the bifunctional cells (an IDC platinum composition at a loading of 8–10 mg/cm<sup>2</sup> on a Ti current collector mesh) so that the electrolyzer performance of Pt could also be measured. More recently a nonreversible Pt/Pt cell, optimized for fuel-cell operation, was built and tested. In this cell the anode and cathode were of the same composition and configuration; the PEM-bonded layers consisted of Pt at a loading of 1 mg/cm<sup>2</sup> with 10 wt.% ionomer, and the free-standing electrodes consisted

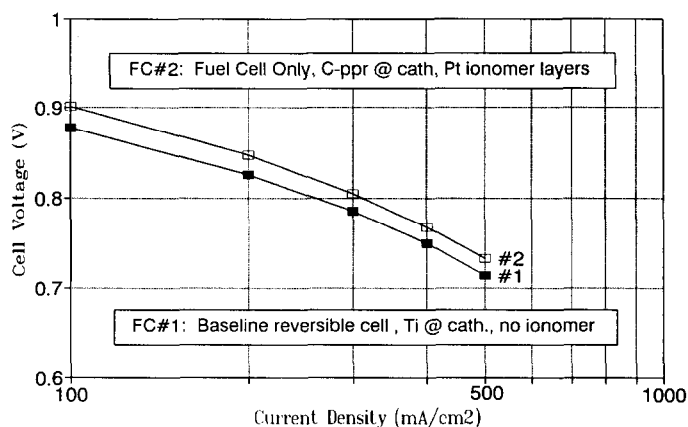


Fig. 1. PEM Pt/Pt fuel cell performance (fuel cell mode only; 80 °C, 30 psi).

of an IDC composition of Pt at a loading of  $4 \text{ mg/cm}^2$  on wet-proofed carbon paper (Toray HO-30). The fuel-cell performance of these two cells is compared in Fig. 1. It can be seen that the cell optimized for fuel-cell operation gave slightly better performance.

#### Baseline Pt/40Pt-60IrO<sub>2</sub> electrolyzer

This cell ran at 1.50 V at  $100 \text{ mA/cm}^2$  and at 1.671 V at  $500 \text{ mA/cm}^2$ . This is fairly typical performance for a dedicated electrolyzer cell with Nafion and Pt/Pt-IrO<sub>2</sub> catalysts. This cell was not tested in fuel cell mode. The performance is presented in Fig. 2 in comparison with the baseline Pt/Pt fuel cell and the baseline Pt/Pt-IrO<sub>2</sub> bifunctional cell.

#### Baseline bifunctional Pt/Pt-IrO<sub>2</sub> cell

Several Pt/Pt-IrO<sub>2</sub> cells with varying IrO<sub>2</sub> contents and electrode structures were evaluated initially to optimize bifunctional performance [6]. A Pt/40Pt-60IrO<sub>2</sub> cell (#5 in Tables 1 and 2) exhibited the best performance in both modes. At  $500 \text{ mA/cm}^2$ , this cell ran at 1.587 V in electrolysis mode and at 0.723 V in fuel cell mode. The comparable voltages for the baseline cells are 1.671 V for the electrolyzer and 0.714 V for the fuel cell. The performance is presented in Fig. 2 in comparison with the baseline Pt/Pt fuel cell and the baseline Pt/Pt-IrO<sub>2</sub> electrolyzer.

#### Catalyst evaluation

##### Bifunctional Pt/Pt-Na<sub>x</sub>Pt<sub>3</sub>O<sub>4</sub> cells

Two different bifunctional cells were constructed for the initial evaluation of Na<sub>x</sub>Pt<sub>3</sub>O<sub>4</sub> as a component of the O<sub>2</sub>-electrode catalyst. The first cell (#6, Na<sub>x</sub>Pt<sub>3</sub>O<sub>4</sub> prep. #21, see Tables 1 and 2) used a two-layer O<sub>2</sub>-catalyst structure bonded to the PEM consisting of very hydrophilic Na<sub>x</sub>Pt<sub>3</sub>O<sub>4</sub> (10% ionomer) and a less hydrophilic Pt transition layer. The balance of the composite electrode was a free-standing IDC electrode consisting of a 33/67 mix of Na<sub>x</sub>Pt<sub>3</sub>O<sub>4</sub> and Pt. This cell gave excellent fuel cell performance ( $0.74 \text{ V}$  at  $500 \text{ mA/cm}^2$ ), as shown in Fig. 2 and Table 2, better than the Pt/Pt cell ( $0.714 \text{ V}$ ) and the best Pt/40Pt-60IrO<sub>2</sub> cell ( $0.723 \text{ V}$ ). The cell

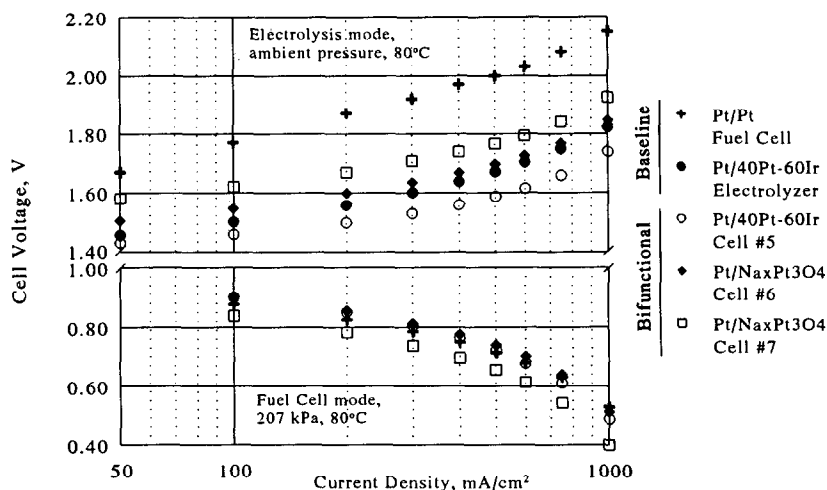


Fig. 2. Performance of bifunctional Pt/Na<sub>x</sub>Pt<sub>3</sub>O<sub>4</sub> PEM cells.

TABLE 2

Cell voltage in fuel cell and electrolysis modes for baseline cells and bifunctional PEM cells; 80 °C, electrolysis at ambient pressure, fuel cell at 207 kPa

Cell performance in --->	Electrolysis mode		Fuel cell mode	
	100 mA/cm <sup>2</sup> (V)	500 mA/cm <sup>2</sup> (V)	100 mA/cm <sup>2</sup> (V)	500 mA/cm <sup>2</sup> (V)
Positive electrode Red./evol. cat.				
Baseline fuel cells				
Pt/Pt (reversible)	1.770	2.000	0.874	0.714
Pt/Pt (fuel cell)	not tested	not tested	0.901	0.733
Baseline electrolyzer				
Pt/40Pt-60IrO <sub>2</sub>	1.500	1.671	not tested	not tested
Bifunctional cells #				
5 Pt/40Pt-60IrO <sub>2</sub>	1.456	1.587	0.901	0.723
6 Pt/Na <sub>x</sub> Pt <sub>3</sub> O <sub>4</sub> -Pt	1.545	1.697	0.903	0.740
7 Pt/Na <sub>x</sub> Pt <sub>3</sub> O <sub>4</sub> -Pt	1.621	1.766	0.839	0.657
8 Pt/40Pt-60IrO <sub>x</sub>	1.477	1.624	0.888	0.704
9 Pt/50RuO <sub>x</sub> -50IrO <sub>x</sub>	1.406	1.627	0.778	0.565
10 Pt/40Pt-60RuO <sub>x</sub>	1.417	1.589	0.784	0.566
11 Pt/RhO <sub>2</sub>		1.675		0.460
12 Pt/40Pt-60IrO <sub>x</sub>	1.489	1.620	0.858	0.640
13 Pt/40Pt-60IrO <sub>x</sub>	1.455	1.550	0.870	0.714
14 Pt/33Pt-67Na <sub>x</sub> Pt <sub>3</sub> O <sub>4</sub>		1.873	0.873	0.698
15 Pt/33Pt-67Na <sub>x</sub> Pt <sub>3</sub> O <sub>4</sub>	1.599	1.797	0.866	0.704
16 Pt/33Pt-67Na <sub>x</sub> Pt <sub>3</sub> O <sub>4</sub>	1.618	1.799	0.838	0.597

performance in electrolysis mode was 1.697 V at 500 mA/cm<sup>2</sup>, better than Pt/Pt (2.00 V), but not as good as the best Pt/40Pt-60IrO<sub>2</sub> cell (1.587 V).

The second Na<sub>x</sub>Pt<sub>3</sub>O<sub>4</sub>-containing bifunctional cell (#7, Na<sub>x</sub>Pt<sub>3</sub>O<sub>4</sub> prep. #34A3) was constructed using a single layer of Na<sub>x</sub>Pt<sub>3</sub>O<sub>4</sub> with 10% ionomer bonded to the PEM and the standard IDC Pt free-standing IDC electrode as the composite O<sub>2</sub> electrode. This cell showed reduced performance in both modes compared with the first Na<sub>x</sub>Pt<sub>3</sub>O<sub>4</sub> cell (Fig. 2 and Table 2). In the fuel-cell mode, the voltage at 500 mA/cm<sup>2</sup> was 0.657 V. In electrolysis mode, the voltage was 1.766 V at 500 mA/cm<sup>2</sup>, which is still a significant improvement over a pure Pt/Pt cell. The differences in performance between these two cells may be partly due to differences in catalytic activity since the materials, although very similar in physical characteristics, are from two separate and somewhat different preparations (see Table 1); a larger part of the differences, however, may be attributed to the changes in electrode structure in cell #7 resulting in a higher resistance interface.

#### *Pt/Pt-IrO<sub>2</sub>*

Cell #8 was an attempt to repeat the build of the baseline bifunctional Pt/Pt-IrO<sub>2</sub> cell (#5) but with two slight differences: slightly more ionomer in the PEM-bonded layer and the introduction of a thin Pt transition layer between the bonded layer and the free-standing electrode. The cell had somewhat higher resistance and did not perform quite as well as cell #5; the performance curves are shown in Fig. 3.

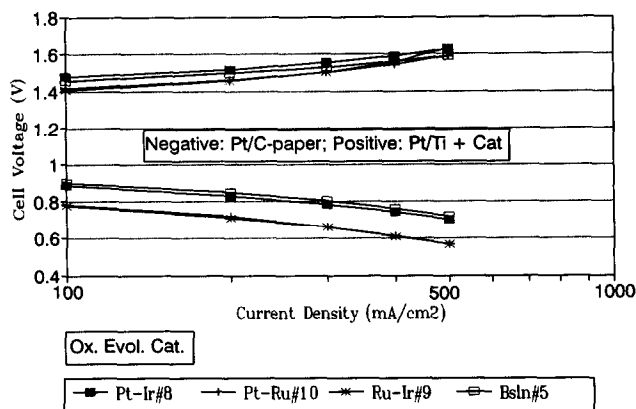


Fig. 3. Bifunctional oxygen catalyst evaluation (Nafion 117, 80 °C, 30 psi).

### $RuO_x-IrO_x$

This alloy was used as the PEM-bonded layer for  $O_2$  evolution in cell #9 and the Pt transition layer was included for comparison to cell #8. The electrolysis performance was better than for cell #8 but the fuel cell performance was not as good (see Fig. 3). It is anticipated that a structural reconfiguration of the cell duplicating cell #5 would significantly upgrade fuel-cell performance with this catalyst.

### $Pt-RuO_x$

This alloy was used as the PEM-bonded layer for  $O_2$  evolution in cell #10 and the Pt transition layer was again included for comparison. The performance was quite similar to the performance observed for  $RuO_x-IrO_x$  (see Fig. 3).

### $RhO_x$

$RhO_x$  was used as the PEM-bonded layer for  $O_2$  evolution in cell #11 but the Pt transition layer was eliminated. This material was difficult to work with because of the very high surface area and more development would be required for a fair evaluation. Two performance points are shown in Table 2, but the cell was not very stable in either mode.

### Repetitive cycling tests

Cells #12 and #13 were attempts to reproduce the electrode structures and performance of the baseline bifunctional Pt/40Pt-60Ir $O_2$  cell (#5) for the purpose of investigating tolerance to repetitive cycling. The first build (#12) had somewhat higher than typical internal resistance and showed lower performance than cell #5 (Table 2). The cell was subjected to six charge/discharge cycles at 500 mA/cm $^2$ , shown in Fig. 4, after which it developed a leak and testing was terminated.

Cell #13 came somewhat closer in performance to cell #5; in fuel-cell mode it was not quite as good as cell #5 but in electrolysis mode it was somewhat better (see Table 2). This build was subjected to 15 charge/discharge cycles, at which point it also developed a leak. The performance at 500 mA/cm $^2$ , shown in Fig. 5, remained fairly constant for both modes of operation over the 15 cycles.

Cells #14, #15 and #16 were attempts to fabricate bifunctional positive electrodes similar to that used in cell #5 but based on  $Na_xPt_3O_4$ , also for the purpose of

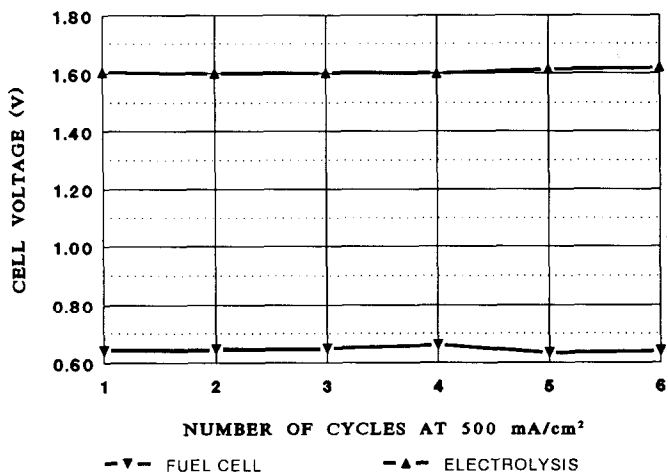


Fig. 4. Cyclic performance of cell #12 (Pt/Pt-IrO<sub>x</sub>, 80 °C); (- ▼ -) fuel cell, and (- ▲ -) electrolysis.

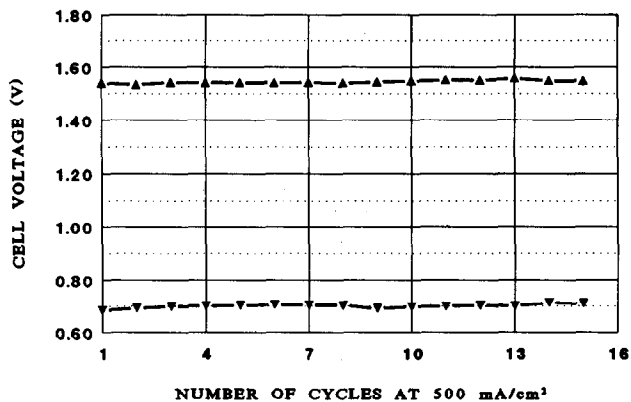


Fig. 5. Cyclic performance of cell #13 (Pt/Pt-IrO<sub>x</sub>, 80 °C); (- ▼ -) fuel cell, and (- ▲ -) electrolysis.

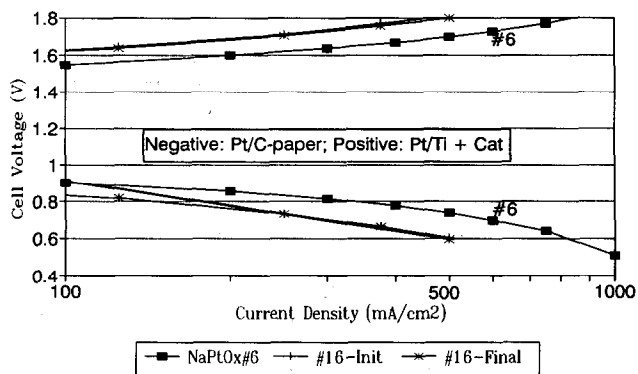


Fig. 6. Cell #16 before and after five cycles (Nafion 117, 80 °C, 30 psi).



investigating tolerance to repetitive cycling. The first two builds (#14 and #15) did not give very stable performance and were not cycled (see Table 2). Cell #16 did not show any significant improvement in performance but was somewhat more stable (Fig. 6) and was subjected to five charge/discharge cycles. Neither the performance of cell #5 nor the performance of the earlier  $\text{Na}_x\text{Pt}_3\text{O}_4$  build (#6) was reproduced, but the cyclic performance was stable and better than Pt alone.

## Conclusions

Regenerative PEM fuel cells showing efficient bifunctional performance can be fabricated with traditional Pt and Pt-Ir catalysts if the electrode structures are properly designed. This investigation has also identified  $\text{RuO}_x$  as a catalyst with good potential for improving the  $\text{O}_2$ -evolution component of a bifunctional positive electrode.  $\text{Na}_x\text{Pt}_3\text{O}_4$  was identified in our earlier work as a catalyst with potential for bifunctional operation in both alkaline and acid electrolytes; the current work has confirmed this with limited charge/discharge cycling but additional development will be required to achieve more reproducible catalyst properties and performance.

## Acknowledgements

This phase of the work was supported by NASA Lewis Research Center under the direction of Dr Patricia Loyselle on Contract No. NAS3-24635. We would also like to acknowledge the assistance of Prof B.L. Chamberland of the University of Connecticut in the selection and identification of numerous materials tested in this program.

## References

- 1 L. Swette and J. Giner, *J. Power Sources*, 22 (1988) 399–408.
- 2 L. Swette and N. Kackley, *J. Power Sources*, 29 (1990) 423–436.
- 3 L. Swette, N. Kackley and S.A. McCatty, *J. Power Sources*, 36 (1991) 323–339.
- 4 L. Swette and N. Kackley, *Proc. 26th Intersociety Energy Conversion Engineering Conf., Boston, MA, USA, Aug. 4–9, 1991*, Vol. 3, 1991, pp. 486–491
- 5 R. Adams and R.L. Shriner, *J. Am. Chem. Soc.*, 45 (1923) 2171–2179.
- 6 L. Swette, N.D. Kackley and A.B. LaConti, *Proc. 27th Intersociety Energy Conversion Engineering Conf., San Diego, CA, USA, Aug. 3–7, 1992*, pp. 1.101–1.106.